Atmos. Chem. Phys. Discuss., 15, 26315–26355, 2015
www.atmos-chem-phys-discuss.net/15/26315/2015/
doi:10.5194/acpd-15-26315-2015

Atmospheric Chemistry and Physics Discussions

Fossil and non-fossil source contributions to atmospheric carbonaceous aerosols during extreme spring grassland fires in Eastern Europe

V. Ulevicius[1], S. Byčenkienė[1], C. Bozzetti[2], A. Vlachou[2], K. Plauškaitė[1], G. Mordas[1], V. Dudoitis[1], G. Abbaszade[3], V. Remeikis[1], A. Garbaras[1], A. Masalaite[1], J. Blees[2], R. Fröhlich[2], K. R. Dällenbach[2], F. Canonaco[2], J. G. Slowik[2], J. Dommen[2], R. Zimmermann[3,4], J. Schnelle-Kreis[3], G. A. Salazar[5], K. Agrios[5,6], S. Szidat[5], I. El Haddad[2], and A. S. H. Prévôt[2]

[1]Department of Environmental Research, SRI Center for Physical Sciences and Technology, Vilnius, Lithuania
[2]Laboratory of Atmospheric Chemistry, Paul Scherrer Institute (PSI), 5232 Villigen, Switzerland
[3]Helmholtz Zentrum München, German Research Center for Environmental Health (GmbH), Joint Mass Spectrometry Centre, Cooperation Group Comprehensive Molecular Analytics and Helmholtz Virtual Institute of Complex Molecular Systems in Environmental Health – Aerosol and Health (HICE), 85764 Neuherberg, Germany

[4]Analytical Chemistry & Joint Mass Spectrometry Centre, Institute of Chemistry, University of Rostock, Dr.-Lorenz-Weg 1, 18051 Rostock, Germany
[5]Department of Chemistry and Biochemistry & Oeschger Centre for Climate Change Research, University of Bern, 3012 Bern, Switzerland
[6]Laboratory of Radiochemistry and Environmental Chemistry, PSI, 5232 Villigen, Switzerland

Received: 15 July 2015 – Accepted: 31 August 2015 – Published: 29 September 2015

Correspondence to: V. Ulevicius (ulevicv@ktl.mii.lt) and A. S. H. Prévôt (andre.prevot@psi.ch)

Published by Copernicus Publications on behalf of the European Geosciences Union.

Abstract

In early spring the Baltic region is frequently affected by high pollution events due to biomass burning in that area. Here we present a comprehensive study to investigate the impact of biomass/grass burning (BB) on the evolution and composition of aerosol in Preila, Lithuania, during springtime open fires. Non-refractory submicron particulate matter (NR-PM_1) was measured by an Aerodyne aerosol chemical speciation monitor (ACSM) and a source apportionment with the multilinear engine (ME-2) running the positive matrix factorization (PMF) model was applied to the organic aerosol fraction to investigate the impact of biomass/grass burning. Satellite observations over regions of biomass burning activity supported the results and identification of air mass transport to the area of investigation. Sharp increases in biomass burning tracers, such as levoglucosan up to 683 ng m^{-3} and black carbon (BC) up to 17 µg m^{-3} were observed during this period. A further separation between fossil and non-fossil primary and secondary contributions was obtained by coupling ACSM PMF results and radiocarbon (^{14}C) measurements of the elemental (EC) and organic (OC) carbon fractions. Non-fossil organic carbon (OC_{nf}) was the dominant fraction of PM_1, with the primary (POC_{nf}) and secondary (SOC_{nf}) fractions contributing 26–44 % and 13–23 % to the TC, respectively. 5–8 % of the TC had a primary fossil origin (POC_f), whereas the contribution of fossil secondary organic carbon (SOC_f) was 4–13 %. Non-fossil EC (EC_{nf}) and fossil EC (EC_f) ranged from 13–24 % and 7–12 %, respectively. Isotope ratio of stable carbon and nitrogen isotopes were used to distinguish aerosol particles associated with solid and liquid fossil fuel burning.

1 Introduction

On global scale wood or grass burning is a major source of organic aerosol (Crutzen et al., 1979; Levine, 1996). Approximately 90 % of vegetation burning is caused by human-induced fires (Baldini et al., 2002) and only a minor fraction derives from nat-

ACPD
15, 26315–26355, 2015

ural processes such as lightning. The composition of biomass smoke depends on the type of wood, combustion conditions (flaming vs. smoldering), and ambient weather conditions (Weimer et al., 2008; Grieshop et al., 2009; Hawkins and Russell, 2010; Akagi et al., 2012). Fine particles emitted from biomass burning include directly emitted primary particles (POA) and secondary organic aerosols (SOA), formed in the atmosphere as the plume ages through photochemical processes driven by sunlight (Capes et al., 2008; Heringa et al., 2011).

Many studies have revealed that organic matter (OM) is the largest fraction of ambient fine particles, typically comprising 20–90 % of the submicron particulate mass (Jimenez et al., 2009). Factor analysis of aerosol mass spectra from Aerodyne aerosol mass spectrometer enables the deconvolution of OM into different factors based on their mass spectral fingerprints (Lanz et al., 2007; Aiken et al., 2009; Ulbrich et al., 2009). Such results provided valuable insights into the source and transformation processes of organic aerosols (OA) in the atmosphere (Lanz et al., 2010; Ng et al., 2011; Hildebrandt et al., 2011; Canonaco et al., 2013; Bougiatioti et al., 2014; Huang et al., 2014).

The main type of biomass burning in Lithuania and surrounding countries in early spring during the last years is illegal *grass burning* for land clearing (Ulevicius et al., 2010b; Byčenkienė et al., 2013). The north-east European countries are considered to influence significantly the microphysical, chemical and optical properties of the aerosol in the Baltic Sea region (Kikas et al., 2008; Zawadzka et al., 2013; Mann et al., 2014; Beddows et al., 2014). Long-term measurements of carbonaceous aerosols performed in this area by Ulevicius et al. (2010a, b) and Byčenkienė et al. (2011, 2013) reported a yearly occurrence of high biomass burning organic aerosol (BBOA) levels during March–April related to regional transport from the Kaliningrad region, Ukraine and southwestern part of Russia surrounding the Black Sea, but information on the nature and chemical composition of the biomass burning aerosol in Lithuania is still limited. There has been no systematic investigation of the impact of biomass burning on ambient organic aerosol levels in this region, and a quantitative estimate is needed to

ACPD
15, 26315–26355, 2015

understand the possible impacts of BBOA on air quality in the south-eastern Baltic Sea region.

In many studies levoglucosan was used to assess the contribution of biomass-burning smoke to the aerosol mass concentrations (Puxbaum et al., 2007). A number of source emission studies reported that levoglucosan is not a useful tracer after long-range transport due to its transformation (Hoffmann et al., 2010; Hennigan et al., 2010; Mochida et al., 2010). In contrast to levoglucosan, determination of radiocarbon (^{14}C) offers a unique possibility for source apportionment of carbonaceous aerosol particles, as it unambiguously distinguishes fossil from non-fossil emissions (e.g. Currie, 2000; Ceburnis et al., 2011).

For this study, in the framework of the Lithuanian–Swiss Cooperation Programme joint research project (AEROLIT), an ACSM was deployed in a background area of the South Baltic Sea to measure airborne submicron particles for one month during a period of frequent grass burning pollution. The main findings include investigation of OA components (Sects. 3.1–3.2), molecular markers (Sect. 3.2), source apportionment of EC and OC using ^{14}C data and positive matrix factorization (PMF) of the ACSM organic mass spectra (Sect. 3.3).

2 Methods

2.1 Site description and filter sampling

Continuous air monitoring and time integrated particulate matter sampling were carried out in March 2014 in Preila, Lithuania (55°55′ N, 21°04′ E 5 m a.s.l.) (Fig. 1). Preila is a representative coastal background site, an ideal location for studying the long-range transport of air pollutants in the South-eastern Baltic region due to the absence of significant local sources (Fig. 1, Table 1). It served as a "super site" for the EUSAAR-EU-funded I3 (Integrated Infrastructures Initiatives) project. During the measurement period, strong biomass burning activities were observed on 9–10 March 2014. A high-

ACPD
15, 26315–26355, 2015

volume sampler (500 L min^{-1}) was used to collect PM_1 aerosol particles onto 150 mm diameter Pallflex quartz fibre filters (pre-baked for 24 h at 550 °C). Filters were stored in a freezer (at −20 °C) immediately after sampling.

2.2 Instrumentation

2.2.1 Aerosol Chemical Speciation Monitor and data analysis

An ACSM (Aerodyne Research, Inc., Billerica, MA, USA) was deployed to measure PM_1 components in Preila (Fig. 1, Sect. 2.1). A PM_{10} impactor-type inlet was utilized to remove coarse particles from the sample stream. The sampling air (1.6 L min^{-1}) passed through ~ 2.5 m long stainless steel tube with a 6 mm i.d. and a Nafion dryer (MD-110-48S-4, PermaPure LLC, Toms River, NJ, USA) before reaching the device. Aerosol particle losses in sampling lines were less than 2 % and the relative humidity lower 50 %. The resulting aerosol flow was split and directed to a scanning mobility particle sizer TSI 3936 (TSI Inc., Shoreview, MN, USA) and to the ACSM. In the ACSM particles were directed onto a resistively heated surface at ~ 600 °C where NR-PM_1 components are flash vaporized and the resulting gases are subsequently ionized by 70 eV electron impact. ACSM was operated with a time resolution of ~ 28 min (for typical aerosol loadings, i.e. several µg m^{-3}) and a scan rate of 220 ms amu^{-1} from m/z 10 to 140 (approximately 31.9 s per scan and 1.126 s pause), 56 scans and data interval 30 min. The data acquisition software used was DAQ 1.4.4.4. The mass concentrations and mass spectra were processed using ACSM standard data analysis software (v 1.5.3.0).

The instrument was calibrated using ammonium sulphate and ammonium nitrate. The determined calibration parameters were response factor (RF) $RF_{NO_3} = 2.75 \times 10^{-11}$ and relative ionization efficiency (RIE) $RIE_{NH_4} = 6.16$, $RIE_{SO_4} = 0.92$. The $RIE_{Org} = 1.4$, $RIE_{Chl} = 1.3$ were set as default. The particle counting efficiency depends on the aerosol particle transport efficiency in the sampling line and on the collection efficiency of ACSM. The transport efficiency of the

ACPD
15, 26315–26355, 2015

used sampling line was 0.96 in the aerosol particle size range from 30 nm to 5 µm. However, the ACSM collection efficiency varies depending on the acidity of aerosol particles, aerosol composition, and particle phase water (Matthew et al., 2008). Many atmospheric aerosol studies reported reasonable agreement and linear correlations were obtained with other measurements by using a collection efficiency of 0.5 (Aiken et al., 2009; Timonen et al., 2010). Also, Middlebrook et al. (2012) had proposed the collection efficiency calculation algorithm. The average of collection coefficient of 0.52 was calculated, which is very close to other studies. That is understandable because the sampled aerosol was dryed lower 50 % and the nitrate fraction was quite low. Thus, the resulting instrument particle counting effciency was 0.52. The time series of organic aerosol mass spectra were processed using PMF analysis.

2.2.2 PMF analysis

The ACSM measured data were averaged to 1 h time resolution. A graphical user interface SoFi (Source Finder) (Canonaco et al., 2013), developed at Paul Scherrer Institute was used to perform PMF for the source apportionment of the non-refractory OA mass spectra collected during March 2014. Only signals at $m/z < 120$ were used for PMF analysis (Paatero and Tapper, 1994; Paatero, 1997) due to the following reasons: (1) the signals above $m/z > 120$ account for a minor fraction of total signal, (2) the m/z's > 120 have larger uncertainties because of poor ion transmission and the large interferences of naphthalene signals on some m/z's (e.g., m/z 127, 128, and 129) (Sun et al., 2012). A 2-factor solution including a Primary Organic Aerosol factor (POA), and a Secondary Organic Aerosol factor (SOA) was selected for this study. 20 different PMF runs were performed using a bootstrapping approach (Davison and Hinkley, 1997). The bootstrap creates new input data matrices by randomly resampling measured mass spectra from the original input matrices. Moreover each PMF bootstrap run is initiated from a different pseudorandom starting-point of the algorithm (seed). The bootstrapping approach, together with the seed approach allows a reasonable exploration of the PMF solution space (Paatero et al., 2014). Higher order solutions (3

ACPD
15, 26315–26355, 2015

factors) were explored yielding additional primary profiles, without a significant modification of the secondary contributions. Moreover the retrieved additional profiles showed very high time correlation ($R^2 = 0.98$) with the POA factor, suggesting a splitting of the same aerosol source. As the additional primary factors could not be associated to specific primary emissions, those solutions are not shown. Medium-long range transport of polluted air masses resulted in a co-variability of the sources at the sampling site, hampering a further separation of the primary organic aerosols.

2.2.3 7-wavelength aethalometer

An aethalometer, Model AE31 Spectrum (Manufactured by Aerosol d.o.o., Ljubljana, Slovenia) provided continuous measurements of the BC mass concentrations. The aethalometer was equipped with a $PM_{2.5}$ impactor. The aethalometer data were recorded with a 5 min time resolution. The optical transmission of light absorbing carbonaceous aerosol particles was measured at seven wavelengths (370, 450, 520, 590, 660, 880, and 950 nm). Measurements at 880 nm wavelength were used to determine BC mass concentration (Lavanchy et al., 1999). The aethalometer converts light attenuation measurements to BC mass using specific attenuation absorption cross-section (σ) of 16.6 $m^2 g^{-1}$ (at 880 nm) (Aethalometer Operations manual). The default value for a near-infrared wavelength of 880 nm was set by the manufacturer. An empirical algorithm for loading effects compensation was used (Collaud Coen et al., 2010).

2.2.4 OC/EC, ^{14}C, $\delta^{13}C$ and $\delta^{15}N$ analysis

Filter measurements were performed to determine OC, EC and TC concentrations with a thermo-optical OC/EC analyser (Sunset Laboratory Inc, USA) equipped with a non-dispersive infrared (NDIR) detector. A 1.5 cm^2 filter punch was analysed according to the EUSAAR2 protocol (Cavalli et al., 2010). The blank filter was subtracted only from the measured OC and TC concentrations, as for the EC the corresponding blank was below the detection limits of the instruments.

ACPD
15, 26315–26355, 2015

^{14}C in EC and TC was measured using the accelerator mass spectrometer MICADAS, equipped with a gas-capable ion source (Szidat et al., 2014). ^{14}C analysis of TC was determined after combustion of filter punches in an elemental analyser, directly coupled to the MICADAS (Salazar et al., 2015). The TC ^{14}C raw data were corrected for a representative field blank. For ^{14}C analysis of EC, the filters were first water extracted in order to minimize charring by removing the water-soluble OC (WSOC). Then the Swiss_4S protocol (Zhang et al., 2012) was used to remove the water-insoluble OC (WINSOC) and measure the EC ^{14}C, by coupling of the Sunset instrument to the MICADAS (Agrios et al., 2015). ^{14}C in OC was determined from the TC ^{14}C and the EC ^{14}C results with an isotope mass balance calculation. All the data from the ^{14}C analysis were corrected for the decay of the ^{14}C from 1950 until present. The reported uncertainty for the non-fossil fraction of EC includes both charring of OC (overestimation of EC) and EC loss (underestimation of EC) during the WINSOC removal process (Zhang et al., 2012). Non-fossil fractions of TC, EC and OC (i.e., TC_{nf}, EC_{nf} and OC_{nf}) were determined from the individual ^{14}C analyses and ^{14}C reference values. These reference values represent emissions from purely non-fossil sources and amount 1.06 ± 0.03 for TC and OC and 1.10 ± 0.03 for EC based on the calculation of Mohn et al. (2008). The fossil fractions of TC, EC and OC (i.e., TC_f, EC_f and OC_f) were determined by subtraction of the respective non-fossil fractions.

Bulk $\delta^{13}C$ and $\delta^{15}N$ values were derived by measuring filter pieces (1.4 cm^2) wraped in tin capsules (8×5 mm, Elemental Microanalysis) using an elemental analyser accompanying an isotope ratio mass spectrometer (EA-IRMS, Flash EA1112 – Thermo V Advantage) via a ConFlo III interface. The autosampler of the EA was continuously flushed with He (180 mL min^{-1}) to remove all atmospheric gases. Helium flow on the oxidation column was 80 mL min^{-1}. Flash combustion occurred in the oxidation column with the presence of O_2 (the O_2 flow was 180 mL min^{-1} for 4 s). Formed gases were taken to the reduction column in which molecular nitrogen was obtained from any nitrogen oxides followed by a water trap (magnesium perchlorate). The nitrogen and the carbon dioxide were separated on a packed gas chromatographic (GC) column (Po-

ACPD
15, 26315–26355, 2015

raPlot, 3 cm × 2 cm, 35 °C) and delivered to the isotope ratio mass spectrometer (via the ConFlo interface) where the measurement of carbon and nitrogen isotope ratio was made. The amount of nitrogen and carbon in the sample was determined by a thermal conductivity detector which is a part of the elemental analyser. These measurements were used in the isotope mass balance calculations (Eq. 1).

The total carbon and total nitrogen fractions of the aerosol particles were used for the isotopic ratio measurements. Stable carbon and nitrogen isotopic ratio measurements were expressed relative to the Vienna Pee Dee Belemnite (VPDB) standard using the formula:

$$\delta^{13}\mathrm{C} = (\mathrm{R}_{\mathrm{sample}}/\mathrm{R}_{\mathrm{standard}} - 1) \cdot 1000\,(‰), \quad (1)$$

where R_{sample} and R_{standard} are the ratios of ^{13}C to ^{12}C (or ^{15}N to ^{14}N) in the sample and the standard (referred to as VPDB), respectively.

Repeated analysis of certified reference material (caffeine IAEA-600) and oil (NBS 22) gave an average δ^{13}C value: mean $\pm\sigma = -27.77 \pm 0.08$ ‰ (certified value: mean $\pm\sigma = -27.771 \pm 0.043$ ‰ $_{\mathrm{VPDB}}$) and $\delta^{13}\mathrm{C} = -30.031 \pm 0.043$ ‰$_{\mathrm{VPDB}}$ respectively. These values were used for δ^{13}C measurements in order to evaluate an analytical precision and calibration of a reference gas (CO_2) to VPDB. Meanwhile, the IAEA-600 standard gave an average δ^{15}N value: mean $\pm\sigma = 1 \pm 0.2$ ‰ which was used for calibration of a reference gas (N_2) to air (for δ^{15}N measurements).

Stable carbon and nitrogen isotope ratios were measured in the samples with the signal intensity reaching 1000 mV or more, due to analytical restrictions (the isotope values measurements below 1000 mV did not fulfil linearity requirements of 0.07 ‰ V^{-1} for the internal standard).

The mass balance equation was used to calculate the real δ values of carbon or nitrogen of the aerosol samples (blank correction):

$$m_{\mathrm{measured}} \times \delta X_{\mathrm{measured}} = m_1 \times m_{\mathrm{blank}} \times \delta X_{\mathrm{blank}}, \quad (2)$$

ACPD
15, 26315–26355, 2015

where $m_{measured}$ was the mass of measured material (carbon or nitrogen) in the measured sample, $\delta X_{measured}$ was the measured (aerosol + filter) δ value (carbon or nitrogen), m_1 was the mass of pure material (carbon or nitrogen), and m_{blank} and δX_{blank} were the mass and isotope ratio (of carbon or nitrogen) of the blank filter, respectively.

2.2.5 Radiocarbon-based source apportionment of carbonaceous aerosols

An estimate of fossil and non-fossil primary and secondary organic carbon (POC_f, POC_{nf}, SOC_f, SOC_{nf}) was achieved by coupling ACSM-PMF results, ^{14}C data, and organic marker measurements using a chemical mass balance-like approach. The sensitivity of POC_f, POC_{nf}, SOC_f, and SOC_{nf} contributions to the assumed parameters and measurement errors are described in details in this section. The approach is based on the POC_{nf} estimate, for a subsequent determination of SOC_{nf}, SOC_f, and POC_f as follows:

$$SOC_{nf} = OC_{nf} - POC_{nf} \quad (3)$$

$$SOC_f = SOC - SOC_{nf} \quad (4)$$

$$POC_f = OC_f - SOC_f \quad (5)$$

^{14}C measurements and ACSM-PMF results were coupled as follows for the estimate of POC_{nf} contribution: OC_{nf} results provide an upper boundary for the total POC_{nf} contribution, while POA from ACSM-PMF results provide another upper boundary for POC_{nf}. By combining ^{14}C and PMF results a possible range of POC_{nf} contributions can be obtained. For the sensitivity analysis we considered a uniform distribution of possible POC_{nf} contributions in this range, meaning that each POC_{nf} value in this range was considered as equally probable. For the statistical analysis we retained only the solutions matching the selected acceptance criteria described in the following. From the acceptable solutions we then derived the probability distribution function of the different POC_f, SOC_{nf}, SOC_f, POC_f fractions.

ACPD
15, 26315–26355, 2015

Each POC_{nf} value is associated to a specific levoglucosan/POC_{nf} and EC_{nf}/POC_{nf} ratio. In this manner we determined a probability distribution function of the levoglucosan/POC_{nf} and EC_{nf}/POC_{nf} ratios relative to our acceptable solutions. The assumption that each input POC_{nf} contribution in the selected possible range is equally probable (hereafter referred to as "uniform distribution approach") has advantages and drawbacks: while this assumption does not consider any a priori information about levoglucosan/POC_{nf} and EC_{nf}/POC_{nf}, it considers those ratios as equally possible. To explore the influence of this assumption on our results we performed the same sensitivity analysis assuming an input levoglucosan/POC_{nf} distribution derived from 33 profiles for combustion of hard or softwoods in domestic fireplaces or woodstoves (Fine et al., 2001, 2002, 2004a, b; Schmidl et al., 2008, the approach is hereafter referred to as "non-uniform distribution approach"). We eventually derived the probability distribution functions of the levoglucosan/POC_{nf} and EC_{nf}/POC_{nf} ratios relative to the acceptable solutions. The two approaches provided similar results. From the uniform distribution approach, a median levoglucosan/POC_{nf} ratio of 0.18 (1st quartile = 0.14; 3rd quartile = 0.23) and a median EC_{nf}/POC_{nf} ratio of 0.32 (1st quartile = 0.28; 3rd quartile = 0.36) were retrieved, whilst from the non-uniform distribution approach a median levoglucosan/POC_{nf} ratio of 0.15 (1st quartile = 0.13; 3rd quartile = 0.18) and a median EC_{nf}/POC_{nf} ratio of 0.33 (1st quartile = 0.28; 3rd quartile = 0.36) were obtained.

In the following section a technical description of the sensitivity analysis implementation is reported. For each filter sample i, 10 000 random combinations (r) of input data, $[TC]_{i,r}$, $[EC]_{i,r}$, $[EC_f]_{i,r}$, $[OC_f]_{i,r}$, and $[Levoglucosan]_{i,r}$, were generated. In this process, we assume a normal distribution of the errors around the average $[X]_i$ value (X being one of the input values mentioned above), and a distribution width equal to the standard deviation $\sigma[X]_i$:

For each random combination of input data, the corresponding $[OC]_{i,r}$, $[EC_{nf}]_{i,r}$, and $[OC_{nf}]_{i,r}$ values were determined as:

$$[OC]_{i,r} = [TC]_{i,r} - [EC]_{i,r}, \quad (6)$$

ACPD
15, 26315–26355, 2015

$$[EC_{nf}]_{i,r} = [EC]_{i,r} - [EC_f]_{i,r}, \quad (7)$$

$$[OC_{nf}]_{i,r} = [OC]_{i,r} - [OC_f]_{i,r}. \quad (8)$$

10 000 random $[SOC]_s$ values were generated by randomly selecting a daily average $[SOA]_s$ value from one of the 20 ACSM-PMF runs (s). The corresponding $[SOC]_s$ values were derived as:

$$[SOC]_s = [SOA]_s/(OM/OC)_{SOA(s)} \quad (9)$$

$(OM/OC)_{SOA(s)}$ and σ $(OM/OC)_{SOA(s)}$ were calculated according to Aiken et al. (2009) as function of the fractional contribution of the m/z 44 (*f44*) to the SOA_s mass spectra. Fröhlich et al. (2015) showed a systematic difference between *f44* measured from ACSM and AMS, therefore an empirical correction factor was accordingly applied to rescale *f44* from ACSM ($f44_{ACSM}$) data to the corresponding AMS *f44* value ($f44_{AMS}$). The uncertainty relative to the *f44* correction factor was propagated into σ $(OM/OC)_{SOA(s)}$ which includes the O/C_s uncertainty as well. Each $[SOC]_{i,r}$ value was obtained by randomly varying $[SOC]_s$ assuming a normal distribution of errors around the average value $[SOC]_s$ and a distribution width equals σ $(OM/OC)_{SOA(s)}$. $[BBOC]_{i,r}$ contributions for each sample*i* were derived as follows:

$$[BBOC]_{i,r} = [levoglucosan]_{i,r}/\alpha, \quad (10)$$

$$[BBOC]_{i,r} = [EC_{nf}]_{i,r}/\beta, \quad (11)$$

where α represents the levoglucosan/BBOC ratio. This ratio was systematically varied between 0.01 and 0.31 according to Huang et al. (2014) and references therein (scan step equals 0.01). β corresponds to the EC/BBOC ratio. Values of β were systematically varied between 0.1 and 0.4 according to Zhang et al. (2015) and references therein (scan step equals 0.01). 10 000 $[BBOC]_{i,r,\alpha}$ and 10 000 $[BBOC]_{i,r,\beta}$ were determined as in Eqs. (8) and (9). Only acceptable $[BBOC]_{i,r,\alpha/\beta}$ (= $[POC_{nf}]_{i,r,\alpha/\beta}$) values

ACPD
15, 26315–26355, 2015

were considered for the sensitivity analysis. The criteria to consider a $[BBOC]_{i,r,\alpha/\beta}$ value as acceptable were:

(a) $[BBOC]_{i,r,\alpha/\beta} \leq [POC]_{i,r}$ and (b) $[BBOC]_{i,r,\alpha/\beta} \leq [OC_{nf}]_{i,r}$ (12)

$[POC]_{i,r}$ was determined as follows:

$$[POC]_{i,r} = [OC]_{i,r} - [SOC]_{i,r}, \quad (13)$$

Only acceptable $[POC]_{i,r}$ values were considered. The criterion to consider a $[POC]_{i,r}$ value as acceptable was:

(c) $[POA]_s/[POC]_{i,r} \geq 1.3$ according to Mohr et al. (2009), Aiken et al. (2009).

$[SOC_{nf}]_{i,r}$ values were then derived as:

$$[SOC_{nf}]_{i,r} = [OC_{nf}]_{i,r} - [POC_{nf}]_{i,r} \quad (14)$$

Only acceptable $[SOC_{nf}]_{i,r}$ values were considered, where

(d) $[SOC_{nf}]_{i,r} \leq [SOC]_{i,r}$. (15)

Only solutions where all 4 criteria (a), (b), (c), and (d) held were considered acceptable and retained.

Finally, $[SOC_f]_{i,r}$ and $[POC_f]_{i,r}$ were calculated as:

$$[SOC_f]_{i,r} = [SOC]_{i,r} - [SOC_{nf}]_{i,r}, \quad (16)$$

$$[POC_f]_{i,r} = [OC_f]_{i,r} - [SOC_f]_{i,r}. \quad (17)$$

2.2.6 Satellite products and organic markers

Determination of organic marker concentrations were performed using a recently developed in-situ derivatization thermal desorption gas chromatography time of flight mass spectrometry (IDTD-GC-MS) method (Orasche et al., 2011).

ACPD
15, 26315–26355, 2015

Biomass burning episodes were explored using a variety of remote sensing datasets and their derived properties. Satellite data and ground based observations of aerosol properties from the MODIS, HYSPLIT and SILAM were coupled to analyse the variability of carbonaceous aerosols in Lithuania (Fig. 2).

The MODIS sensors on-board NASA's Terra and Aqua satellites provides multiple thermal observations of the Earth on 9–10 March 2014 at a spatial resolution of 1 km using the latest version of the MODIS Active Fire Product (MOD14/MYD14) algorithm (MODIS, 2011). To identify the influence of air masses from different transport pathways on the large BB event occurring at Preila, 72 h back trajectories at an arrival height of 100, 200 and 500 m were calculated by Hybrid Single Particle Lagrangian Integrated Trajectory (HYSPLIT) Model Version 4.8. All air mass back trajectories were generated using Gridded Meteorological Data archives of the Air Resource Laboratory (ARL), National Ocean and Atmospheric Administration (NOAA) (Fig. 2a).

The Navy Aerosol Analysis and Prediction System (NAAPS) model results were used to define the distribution of BB aerosols from wildfires area (model description and results are available from the web pages of the Naval Research Laboratory, Monterey, CA, USA; http://www.nrlmry.navy.mil/aerosol/) (Fig. 2b). The NAAPS model has been adapted to combine real-time observations of biomass burning based on the joint Navy/NASA/NOAA Fire Locating and Modelling of Burning Emissions system (FLAMBE, http://www.nrlmry.navy.mil/flambe/) (Reid et al., 2004). The method has proven helpful in previous studies of long-range and regional transport of smoke (Honrath et al., 2004). The resolution of 2.5° longitude × 2.5° latitude National Centers for Environmental Prediction (NCEP) reanalysis data (Kanamitsu et al., 2002) during grass burning episode were analysed to illustrate the sub synoptic-scale weather feature among the biomass burning events over Lithuania issued every 6 h for March 2014 (Fig. 2c). SILAM is an air quality and emergency open code system (http://silam.fmi.fi/) providing $PM_{2.5}$ emission maps by Eulerian dynamics and a combination of basic acid and ozone chemistry with inert particles for fire and anthropogenic primary PM emission to account for the fire induced aerosol contribution (Fig. 2d).

ACPD
15, 26315–26355, 2015

3 Results and discussion

3.1 Identification of grass burning event

Massive active fires occurred throughout the Kaliningrad region (Russia), Belorussia and Ukraine (Fig. 2a) when a high atmospheric pressure system was situated over the study area, as illustrated in the weather map of Fig. 2c. The plumes from those fires covered a large area south of the Baltic region and were transported thousands of kilometres downwind affecting the background air in Lithuania (Fig. 2). Although the number of fires was similar to that one of previous years, the impact of the fire events on the Lithuanian air quality was enhanced in March 2014 due to air mass transport of smoke entrained in deep convection by the large scale circulation around the pressure maximum of the anticyclonic system (Fig. 2c). This is consistent with the relatively high concentrations of smoke reaching Preila as predicted by NAAPS (Fig. 2b).

The weather maps showed that the high concentration of pollutants during this BB event was caused by the anticyclonic large-scale movement, which persisted throughout the lower troposphere causing stagnant conditions and extended aerosol residence time.

3.2 Investigation of PM_1 composition and ambient concentrations of organic tracers

The climatic conditions in West Europe as well as in west part of Lithuania are particular, as the moderate warm climate dominating by air mass transport from Atlantic Ocean, leading to higher humidity. Annual mean temperature increases in west–east direction. The average temperature of March was ~ 3–4 °C. During the BB event (9–11 March) combustion products were spread over the study region by the large-scale atmospheric circulation processes. At the beginning of the BB episode, the wind speed was up to $3\,m\,s^{-1}$ on average in the daytime of 9 March, causing weaker dilution of the pollutants while the BC concentration were higher than $12\,\mu g\,m^{-3}$. The average com-

ACPD
15, 26315–26355, 2015

position of NR-PM_1 show similar dominance of organics to previous observations in Europe (e.g. Crippa et al., 2014).

Organic aerosol (46 %, 6.4 $\mu g\,m^{-3}$ ($\sigma = 9.6\,\mu g\,m^{-3}$)) constituted the major fraction of the NR-PM_1 aerosol concentration composition measured by ACSM during the campaign with lower contributions of sulfate (17 %, 2.4 $\mu g\,m^{-3}$ ($\sigma = 2.2\,\mu g\,m^{-3}$)), nitrate (20 %, 2.8 $\mu g\,m^{-3}$ ($\sigma = 3.6\,\mu g\,m^{-3}$)), ammonium (15 %, 2.0 $\mu g\,m^{-3}$ ($\sigma = 1.8\,\mu g\,m^{-3}$)), and chloride (2 %, 0.2 $\mu g\,m^{-3}$ ($\sigma = 0.6\,\mu g\,m^{-3}$)). OA contribution to NR-PM_1 was found to be much higher during the grass burning period (61 %).

Quantification of monosaccharide anhydrides together with OC and EC from 5–14 March are presented in Fig. 3. It is evident that during the event, when grass burning was most intense, the levoglucosan concentration increased up to 680 $ng\,m^{-3}$. That was significantly lower than values reported during extreme event of August 2010 in Moscow – 3100 $ng\,m^{-3}$ (Popovicheva et al., 2014) and are higher than values (220–290 $ng\,m^{-3}$) reported during a major biomass burning episode over northern Europe in Helsinki (Saarikoski et al., 2007), while background values in Nordic rural background sites were found to be 2.1–9.8 $ng\,m^{-3}$ (Yttri et al., 2011). Concentrations of mannosan varied from 3.1 to 68.0 $ng\,m^{-3}$, with a mean value of 19.0 $ng\,m^{-3}$, and concentrations of galactosan varied from 1.0 to 12.0 $ng\,m^{-3}$. Levoglucosan was more weakly correlated with mannosan ($R^2 = 0.73$) throughout the episode and the levoglucosan to mannosan ratio ranged from 7.5 to 28.5, whereas levoglucosan and galactosan exhibited relatively stronger correlation ($R^2 = 0.89$). The levoglucosan to mannosan (L/M), levoglucosan to galactosan (L/G) and levoglucosan to OC (L/OC) ratios have been used before to separate different BB sources (Fabbri et al., 2009; Oanh et al., 2011; Harrison et al., 2012). The average L/M and L/G ratios during BB event were 15.7 and 51.9, respectively. These values are in the order of those L/M ratios reported (2.0–33.3) for grass fires by Oros et al. (2006). It was observed in previous studies, that the L/OC ratio depends on biomass-burning type (Mochida et al., 2010). The observed L to OC ratio in this study was on average 0.08, consistent with values (0.04–0.08) obtained from leaf and grass burnings reported by Sullivan et al. (2008). The OC/EC ratio ranged

ACPD
15, 26315–26355, 2015

from 1.5 to 6.2 being lower on event days (2.4–3.0) indicating an aerosol composition dominated by organic aerosol.

The measured $\delta^{13}C$ values varied from −28.2 to −26.7 ‰. The lowest stable carbon isotope ratio values (−28.5 ‰) were detected during the period with the highest total carbon concentration of 12.2 µg m^{-3} (10 March 2014) and 8.5 µg m^{-3} (9 March 2014). The highest concentration 14.0 µg m^{-3} of nitrogen was detected on 10 March 2014. The nitrogen isotope ratio values varied from +1.0 to +13.0 ‰ (Fig. 4).

Stable carbon and nitrogen isotope ratios values of aerosol particles derived from biomass burning (C3 plants) and liquid fossil fuel are overlapping (Garbaras et al., 2015; Masalaite et al., 2015; Turekian et al., 1998). Coal derived aerosol particles are characterised by higher $\delta^{13}C$ and lower $\delta^{15}N$ values (Fig. 4, solid lines). $\delta^{13}C$ values of aerosol particles during wild grass burning events distinguish in low $\delta^{13}C$ values (Garbaras et al., 2008; Ulevicius et. al. 2010b). The above mentioned distribution of $\delta^{13}C$ and $\delta^{15}N$ values allowed excluding coal burning as main source for aerosol particles at Preila during the investigated event. Aerosol particles with the $\delta^{13}C$ values equal −28 ‰ and below originated mainly from grass burning events. This interpretation of the data is consistent with the the radiocarbon analysis shown below.

3.3 Source apportionment of EC and OC using ^{14}C data

Relative fossil and non-fossil contributions to OC and EC were evaluated using ^{14}C analysis (Szidat et al., 2014) to enable a more detailed source attribution of the carbonaceous aerosol mass. Widely used, two-source simple models (Currie, 2000; Lemire et al., 2002; Lewis et al., 2004; Szidat et al., 2004) can only distinguish fossil from non-fossil TC emissions. Here, carbonaceous aerosol was described to be composed of the following 4 categories: OC_f and EC_f attributed to primary and secondary fossil fuel combustion; and OC_{nf}, and EC_{nf} typically emitted by to primary and secondary biomass burning, cooking, biogenic emissions and non-fossil OC combustion (Table 2, Fig. 5). There was day-to-day variation in the fractional contributions to TC throughout the BB event. The fraction of elemental carbon from biomass burning EC_{bb}

ACPD
15, 26315–26355, 2015

(= EC_{nf}) to total EC was found to be on average 67 ± 3 %. Such high values are unusual and have only been found in wood burning dominated places like villages in Alpine valleys (Zotter et al., 2014). This shows, together with high levels of levoglucosan, that biomass burning contributed to a large extent to OC_{nf} during this event.

PMF analysis of OA spectra resolved two OA components, which are attributed to POA and SOA, whose mass spectra and time series are presented in Fig. 5b, c. Combining these results with the ^{14}C measurements as described in Sect. 2.2.4 shows that the high grass burning pollution event is characterized by a high non-fossil organic compound fraction, which accounts for up to ∼ 90 % of total carbon mass.

SOA showed reasonable correlation ($R^2 = 0.62$) with average NH_4^+ mass concentration during the BB event. NH_4^+ is in this case a good tracer for secondary aerosol, as it correlates well with the sum of NO_3^- and SO_4^{2-} ($R^2 = 0.96$; linear fit: $y = 0.816 + 0.005$). There was day-to-day variation throughout the study period with the non-fossil contribution to organic carbon between 67–86 %. OC_{nf} was estimated to be ∼ 65 % primary, while the primary fraction of the OC_f in Preila was estimated to be ∼ 93 %. Conversely, when EC_f showed a lower contribution (7 and 10 March 2014; 26 and 24 %, respectively), OC_f was also lower (15 %) (Table 3). The high fraction of biomass burning was corroborated by measurements of levoglucosan. The combination of both techniques allowed a better characterization of the carbonaceous aerosol sources. POA determined with the ACSM is mostly non-fossil and originates from grass burning. The lines in Fig. 6 represent the absolute contribution of each source during 5–10 March 2014. It is shown that POC_{nf} and SOC_{nf} concentrations increase drastically (from 1.1 to 5.4 $\mu g\,m^{-3}$ for POC_{nf}; from 0.9 to 3.1 $\mu g\,m^{-3}$ for SOC_{nf}) with increasing influence of biomass burning, whereas the concentrations of the respective fossil fractions show a smaller increase during this episode. From the acceptable solutions obtained from the sensitivity test described in Sect. 2.2.7, we derived the probability distribution functions of the different daily contributions for POC_f, SOC_{nf}, SOC_f, POC_f fractions (Fig. 6). The median Levoglucosan/BBOC and EC/BBOC ratios obtained from the sensitivity

ACPD
15, 26315–26355, 2015

tests is consistent with values reported in Zhang et al. (2015) and Huang et al. (2014) (Fig. 7).

In Zhang et al. (2015) agricultural waste combustion is considered to be the main contributor to the total biomass burning. Note that on 5 March a different Levoglucosan/BBOC ratio was found (0.31) compared to the rest of the event (~ 0.15). This may mean that a different type of wood burning took place. Also, this is consistent with different wind back-trajectories, associated to air masses originating in the Southern and Central Russian Federal districts, i.e. air masses with a different geographical origin and associated to potentially different types of biomass burning. During the intensive grass burning episode, consecutive new particle formation (NPF) episodes were observed. Observed NPF could be attributed to the grass burning and secondary biomass burning product transformation as was evaluated in earlier studies over same area (Ulevicius et al., 2010b). Similarly, at the same site Ulevicius et al. (2002) observed nucleation events on days when the average daily concentrations of SO_2 or NO_2 were two to three times higher than the average monthly concentrations.

4 Conclusions

In March 2014, an intensive field campaign was conducted in the marine background of South Eastern Baltic region during a period of intensive grass burning. This paper provides the biomass burning related aerosol concentrations during grass burning estimated by data that stem from a synthesis of various techniques including surface online/offline and satellite based measurements. Lidar vertical profiles allowed confirming smoke plume from wild fire regions. Levels of source specific tracers, i.e. levoglucosan as well as ^{14}C of TC, EC and OC have been used as input for source apportionment of the carbonaceous aerosol approach. Overall, EC and OC were dominated by non-fossil sources. The total POC fraction was separated into POC_f and POC_{nf}. In term of OC mass, POC_{nf} contributes on average 56 %, while relative contribution to TC was found to be on average 39 %. In case of SOC, the contribution of OC_f reached on average

ACPD
15, 26315–26355, 2015

10.3 % (non-fossil – 25 %). The $\delta^{13}C$ value of −28.5 % indicated the dominance of the aerosol derived from the vegetation burning as no significant carbon isotope fractionation occurs between the aerosol particles from biomass burning and the raw biomass material.

Acknowledgements. This work was supported by the Lithuanian–Swiss Cooperation Programme "Research and Development" project AEROLIT (Nr. CH-3-ŠMM-01/08).

References

Agrios, K., Salazar, G. A., Zhang, Y. L., Battaglia, M., Luginbühl, M., Ciobanu, V. G., Vonwiller, M., and Szidat, S.: Online coupling of pure O_2 thermo optical methods – ^{14}C AMS for carbonaceous aerosols source apportionment study, Nucl. Instrum. Meth. B., in press, doi:10.1016/j.nimb.2015.06.008, 2015.

Aiken, A. C., Salcedo, D., Cubison, M. J., Huffman, J. A., DeCarlo, P. F., Ulbrich, I. M., Docherty, K. S., Sueper, D., Kimmel, J. R., Worsnop, D. R., Trimborn, A., Northway, M., Stone, E. A., Schauer, J. J., Volkamer, R. M., Fortner, E., de Foy, B., Wang, J., Laskin, A., Shutthanandan, V., Zheng, J., Zhang, R., Gaffney, J., Marley, N. A., Paredes-Miranda, G., Arnott, W. P., Molina, L. T., Sosa, G., and Jimenez, J. L.: Mexico City aerosol analysis during MILAGRO using high resolution aerosol mass spectrometry at the urban supersite (T0) – Part 1: Fine particle composition and organic source apportionment, Atmos. Chem. Phys., 9, 6633–6653, doi:10.5194/acp-9-6633-2009, 2009.

Akagi, S. K., Craven, J. S., Taylor, J. W., McMeeking, G. R., Yokelson, R. J., Burling, I. R., Urbanski, S. P., Wold, C. E., Seinfeld, J. H., Coe, H., Alvarado, M. J., and Weise, D. R.: Evolution of trace gases and particles emitted by a chaparral fire in California, Atmos. Chem. Phys., 12, 1397–1421, doi:10.5194/acp-12-1397-2012, 2012.

Baldini, G., Campadelli, P., and Fradegrada, M.: Biomass burning monitoring by scene analysis, in: Proceedings of Visualization, Imaging, and Image Processing, Calgary, 9–12 September 2002, p. 312–317, 2002.

Beddows, D. C. S., Dall'Osto, M., Harrison, R. M., Kulmala, M., Asmi, A., Wiedensohler, A., Laj, P., Fjaeraa, A.M., Sellegri, K., Birmili, W., Bukowiecki, N., Weingartner, E., Baltensperger, U., Zdimal, V., Zikova, N., Putaud, J.-P., Marinoni, A., Tunved, P., Hansson, H.-C.,

ACPD
15, 26315–26355, 2015

Fiebig, M., Kivekäs, N., Swietlicki, E., Lihavainen, H., Asmi, E., Ulevicius, V., Aalto, P. P., Mihalopoulos, N., Kalivitis, N., Kalapov, I., Kiss, G., de Leeuw, G., Henzing, B., O'Dowd, C., Jennings, S. G., Flentje, H., Meinhardt, F., Ries, L., Denier van der Gon, H. A. C., and Visschedijk, A. J. H.: Variations in tropospheric submicron particle size distributions across the European continent 2008–2009, Atmos. Chem. Phys., 14, 4327–4348, doi:10.5194/acp-14-4327-2014, 2014.

Bougiatioti, A., Stavroulas, I., Kostenidou, E., Zarmpas, P., Theodosi, C., Kouvarakis, G., Canonaco, F., Prévôt, A. S. H., Nenes, A., Pandis, S. N., and Mihalopoulos, N.: Processing of biomass-burning aerosol in the eastern Mediterranean during summertime, Atmos. Chem. Phys., 14, 4793–4807, doi:10.5194/acp-14-4793-2014, 2014.

Byčenkiene, S., Ulevicius, V., and Kecorius, S.: Characteristics of black carbon aerosol mass concentration over the East Baltic region from two-year measurements, J. Environ. Monitor., 13, 1027–1038, doi:10.1039/C0EM00480D, 2011.

Byčenkienė, S., Ulevicius, V., Dudoitis, V., and Pauraitė, J.: Identification and characterization of black carbon aerosol sources in the East Baltic region, Adv. Meteor., 2013, 380614, doi:10.1155/2013/380614, 2013.

Canonaco, F., Crippa, M., Slowik, J. G., Baltensperger, U., and Prévôt, A. S. H.: SoFi, an IGOR-based interface for the efficient use of the generalized multilinear engine (ME-2) for the source apportionment: ME-2 application to aerosol mass spectrometer data, Atmos. Meas. Tech., 6, 3649–3661, doi:10.5194/amt-6-3649-2013, 2013.

Capes, G., Johnson, B., McFiggans, G., Williams, P. I., Haywood, J., and Coe, H.: Aging of biomass burning aerosols over West Africa: aircraft measurements of chemical composition, microphysical properties, and emission ratios, J. Geophys. Res.-Atmos., 113, D00C15, doi:10.1029/2008JD009845, 2008.

Cavalli, F., Viana, M., Yttri, K. E., Genberg, J., and Putaud, J.-P.: Toward a standardised thermal-optical protocol for measuring atmospheric organic and elemental carbon: the EUSAAR protocol, Atmos. Meas. Tech., 3, 79–89, doi:10.5194/amt-3-79-2010, 2010.

Ceburnis, D., Garbaras, A., Szidat, S., Rinaldi, M., Fahrni, S., Perron, N., Wacker, L., Leinert, S., Remeikis, V., Facchini, M. C., Prevot, A. S. H., Jennings, S. G., Ramonet, M., and O'Dowd, C. D.: Quantification of the carbonaceous matter origin in submicron marine aerosol by ^{13}C and ^{14}C isotope analysis, Atmos. Chem. Phys., 11, 8593–8606, doi:10.5194/acp-11-8593-2011, 2011.

ACPD
15, 26315–26355, 2015

Collaud Coen, M., Weingartner, E., Apituley, A., Ceburnis, D., Fierz-Schmidhauser, R., Flentje, H., Henzing, J. S., Jennings, S. G., Moerman, M., Petzold, A., Schmid, O., and Baltensperger, U.: Minimizing light absorption measurement artifacts of the Aethalometer: evaluation of five correction algorithms, Atmos. Meas. Tech., 3, 457–474, doi:10.5194/amt-3-457-2010, 2010.

Crippa, M., Canonaco, F., Lanz, V. A., Äijälä, M., Allan, J. D., Carbone, S., Capes, G., Ceburnis, D., Dall'Osto, M., Day, D. A., DeCarlo, P. F., Ehn, M., Eriksson, A., Freney, E., Hildebrandt Ruiz, L., Hillamo, R., Jimenez, J. L., Junninen, H., Kiendler-Scharr, A., Kortelainen, A.-M., Kulmala, M., Laaksonen, A., Mensah, A. A., Mohr, C., Nemitz, E., O'Dowd, C., Ovadnevaite, J., Pandis, S. N., Petäjä, T., Poulain, L., Saarikoski, S., Sellegri, K., Swietlicki, E., Tiitta, P., Worsnop, D. R., Baltensperger, U., and Prévôt, A. S. H.: Organic aerosol components derived from 25 AMS data sets across Europe using a consistent ME-2 based source apportionment approach, Atmos. Chem. Phys., 14, 6159–6176, doi:10.5194/acp-14-6159-2014, 2014.

Crutzen, P. J., Heidt, L. E., Krasnec, J. P., Pollock, W. H., and Seiler, W.: Biomass burning as a source of atmospheric gases CO, H_2, N_2O, NO, CH_3Cl, and COS, Nature, 282, 253–256, doi:10.1038/282253a0, 1979.

Currie, L. A.: Evolution and multidisciplinary frontiers of ^{14}C aerosol science, Radiocarbon, 42, 115–126, 2000.

Davison, A. C. and Hinkley, D. V.: Bootstrap Methods and Their Application, Cambridge University Press, Cambridge, UK, 582 pp., 1997.

Fabbri, D., Torri, C., Simoneit, B., Marynowski, L., Rushdi, A., and Fabianska, M.: Levoglucosan and other cellulose and lignin markers in emissions from burning of Miocene lignites, Atmos. Environ., 43, 2286–2295, doi:10.1016/j.atmosenv.2009.01.030, 2009.

Fine, P. M., Cass, G. R., and Simoneit, B. R. T.: Chemical characterization of fine particle emissions from fireplace combustion of woods grown in the northeastern United States, Environ. Sci. Technol., 35, 2665–2675, doi:10.1021/es001466k, 2001.

Fine, P. M., Cass, G. R., and Simoneit, B. R. T.: Chemical characterization of fine particle emissions from the fireplace combustion of woods grown in the southern United States, Environ. Sci. Technol., 36, 1442–1451, doi:10.1021/es0108988, 2002.

Fine, P. M., Cass, G. R., and Simoneit, B. R. T.: Chemical characterization of fine particle emissions from the wood stove combustion of prevalent United States tree species, Environ. Eng. Sci., 21, 705–721, doi:10.1089/ees.2004.21.705, 2004a.

ACPD
15, 26315–26355, 2015

Fine, P. M., Cass, G. R., and Simoneit, B. R. T.: Chemical characterization of fine particle emissions fromfireplace combustion of woods grown in the Midwestern and Western United States, Environ. Eng. Sci., 21, 387–409, doi:10.1089/109287504323067021, 2004b.

Fröhlich, R., Crenn, V., Setyan, A., Belis, C. A., Canonaco, F., Favez, O., Riffault, V., Slowik, J. G., Aas, W., Aijälä, M., Alastuey, A., Artiñano, B., Bonnaire, N., Bozzetti, C., Bressi, M., Carbone, C., Coz, E., Croteau, P. L., Cubison, M. J., Esser-Gietl, J. K., Green, D. C., Gros, V., Heikkinen, L., Herrmann, H., Jayne, J. T., Lunder, C. R., Minguillón, M. C., Močnik, G., O'Dowd, C. D., Ovadnevaite, J., Petralia, E., Poulain, L., Priestman, M., Ripoll, A., Sarda-Estève, R., Wiedensohler, A., Baltensperger, U., Sciare, J., and Prévôt, A. S. H.: ACTRIS ACSM intercomparison – Part 2: Intercomparison of ME-2 organic source apportionment results from 15 individual, co-located aerosol mass spectrometers, Atmos. Meas. Tech., 8, 2555–2576, doi:10.5194/amt-8-2555-2015, 2015.

Garbaras, A., Andriejauskiene, J., Bariseviciute, R., and Remeikis, V.: Tracing of atmospheric aerosol sources using stable carbon isotopes, Lith. J. Phys., 48, 259–264, doi:10.3952/lithjphys.48309, 2008.

Garbaras, A., Masalaite, A., Garbariene, I., Ceburnis, D., Krugly, E., Remeikis, V., Puida, E., Kvietkus, K., and Martuzevicius, D.: Stable carbon fractionation in size segregated aerosol particles produced by controlled biomass burning, J. Aerosol Sci., 79, 86–96, doi:10.1016/j.jaerosci.2014.10.005, 2015.

Grieshop, A. P., Logue, J. M., Donahue, N. M., and Robinson, A. L.: Laboratory investigation of photochemical oxidation of organic aerosol from wood fires 1: measurement and simulation of organic aerosol evolution, Atmos. Chem. Phys., 9, 1263–1277, doi:10.5194/acp-9-1263-2009, 2009.

Harrison, R. M., Beddows, D. C. S., Hu, L., and Yin, J.: Comparison of methods for evaluation of wood smoke and estimation of UK ambient concentrations, Atmos. Chem. Phys., 12, 8271–8283, doi:10.5194/acp-12-8271-2012, 2012.

Hawkins, L. N. and Russell, L. M.: Oxidation of ketone groups in transported biomass burning aerosol from the 2008 Northern California Lightning Series fires, Atmos. Environ., 44, 4142–4154, doi:10.1016/j.atmosenv.2010.07.036, 2010.

Hennigan, C. J., Sullivan, A. P., Collett Jr., J. L., and Robinson, A. L.: Levoglucosan stability in biomass burning particles exposed to hydroxyl radicals, Geophys. Res. Lett., 37, L09806, doi:10.1029/2010GL043088, 2010.

ACPD
15, 26315–26355, 2015

Heringa, M. F., DeCarlo, P. F., Chirico, R., Tritscher, T., Dommen, J., Weingartner, E., Richter, R., Wehrle, G., Prévôt, A. S. H., and Baltensperger, U.: Investigations of primary and secondary particulate matter of different wood combustion appliances with a high-resolution time-of-flight aerosol mass spectrometer, Atmos. Chem. Phys., 11, 5945–5957, doi:10.5194/acp-11-5945-2011, 2011.

Hildebrandt, L., Kostenidou, E., Lanz, V. A., Prevot, A. S. H., Baltensperger, U., Mihalopoulos, N., Laaksonen, A., Donahue, N. M., and Pandis, S. N.: Sources and atmospheric processing of organic aerosol in the Mediterranean: insights from aerosol mass spectrometer factor analysis, Atmos. Chem. Phys., 11, 12499–12515, doi:10.5194/acp-11-12499-2011, 2011.

Hoffmann, D., Tilgner, A., Iinuma, Y., and Hermann, H.: Atmospheric stability of levoglucosan: a detailed laboratory and modeling study, Environ. Sci. Technol., 44, 694–699, doi:10.1021/es902476f, 2010.

Honrath, R., Owen, R. C., Val Martin, M., Reid, J., Lapina, K., Fialho, P., Dziobak, M., Kleissl, J., and Westphal, D.: Regional and hemispheric impacts of anthropogenic and biomass burning missions on summertime CO and O_3 in the North Atlantic lower free troposphere, J. Geophys. Res., 109, D2431, doi:10.1029/2004JD005147, 2004.

Huang, R.-J., Zhang, Y., Bozzetti, C., Ho, K.-F., Cao, J.-J., Han, Y., Daellenbach, K. R., Slowik, J. G., Platt, S. M., Canonaco, F., Zotter, P., Wolf, R., Pieber, S. M., Bruns, E. A., Crippa, M., Ciarelli, G., Piazzalunga, A., Schwikowski, M., Abbaszade, G., Schnelle-Kreis, J., Zimmermann, R., An, Z., Szidat, S., Baltensperger, U., El Haddad, I., and Prevot, A. S. H.: High secondary aerosol contribution to particulate pollution during haze events in China, Nature, 514, 218–222, doi:10.1038/nature13774, 2014.

Jimenez, J. L., Canagaratna, M. R., Donahue, N. M., Prevot, A. S. H., Zhang, Q., Kroll, J. H., DeCarlo, P. F., Allan, J. D., Coe, H., Ng, N. L., Aiken, A. C., Docherty, K. S., Ulbrich, I. M., Grieshop, A. P., Robinson, A. L., Duplissy, J., Smith, J. D., Wilson, K. R., Lanz, V. A., Hueglin, C., Sun, Y. L., Tian, J., Laaksonen, A., Raatikainen, T., Rautiainen, J., Vaattovaara, P., Ehn, M., Kulmala, M., Tomlinson, J. M., Collins, D. R., Cubison, M. J., Dunlea, E. J., Huffman, J. A., Onasch, T. B., Alfarra, M. R., Williams, P. I., Bower, K., Kondo, Y., Schneider, J., Drewnick, F., Borrmann, S., Weimer, S., Demerjian, K., Salcedo, D., Cottrell, L., Griffin, R., Takami, A., Miyoshi, T., Hatakeyama, S., Shimono, A., Sun, J. Y., Zhang, Y. M., Dzepina, K., Kimmel, J. R., Sueper, D., Jayne, J. T., Herndon, S. C., Trimborn, A. M., Williams, L. R., Wood, E. C., Middlebrook, A. M., Kolb, C. E., Baltensperger, U., and

ACPD
15, 26315–26355, 2015

Worsnop, D. R.: Evolution of organic aerosols in the atmosphere, Science, 326, 1525–1529, doi:10.1126/science.1180353, 2009.
Kanamitsu, M., Ebisuzaki, W., Woollen, J., Yang, S. K., Hnilo, J. J., Fiorino, M., and Potter, G. L.: NCEP-DOE AMIP-II reanalysis (R-2), B. Am. Meteorol. Soc., 83, 1631–1643, doi:10.1175/BAMS-83-11-1631, 2002.
Kikas, U., Reinart, A., Pugatshova, A., Tamm, E., and Ulevicius, V.: Microphysical, chemical and optical aerosol properties in the Baltic Sea region, Atmos. Res., 90, 211–222, doi:10.1016/j.atmosres.2008.02.009, 2008.
Lanz, V. A., Alfarra, M. R., Baltensperger, U., Buchmann, B., Hueglin, C., and Prévôt, A. S. H.: Source apportionment of submicron organic aerosols at an urban site by factor analytical modelling of aerosol mass spectra, Atmos. Chem. Phys., 7, 1503–1522, doi:10.5194/acp-7-1503-2007, 2007.
Lanz, V. A., Prévôt, A. S. H., Alfarra, M. R., Weimer, S., Mohr, C., DeCarlo, P. F., Gianini, M. F. D., Hueglin, C., Schneider, J., Favez, O., D'Anna, B., George, C., and Baltensperger, U.: Characterization of aerosol chemical composition with aerosol mass spectrometry in Central Europe: an overview, Atmos. Chem. Phys., 10, 10453–10471, doi:10.5194/acp-10-10453-2010, 2010.
Lavanchy, V. M. H., Gaggeler, H. W., Schotterer, U., Schwikowski, M., and Baltensperger, U.: Historical record of carbonaceous particle concentrations from a European high-alpine glacier (Colle Gnifetti, Switzerland), J. Geophys. Res.-Atmos., 104, 21227–21236, doi:10.1029/1999jd900408, 1999.
Lemire, K. R., Allen, D. T., Klouda, G. A., and Lewis, C. W.: Fine particulate matter source attribution for southeast Texas using $^{14}C/^{13}C$ ratios, J. Geophys. Res., 107, 4613, doi:10.1029/2002JD002339, 2002.
Levine, J. S.: Biomass Burning and Global Change, MIT Press, Cambridge, MA, 1996.
Lewis, C. W., Klouda, G. A., and Ellenson, W. D.: Radiocarbon measurement of the biogenic contribution to summertime $PM_{2.5}$ ambient aerosol in Nashville, TN, Atmos. Environ., 38, 6053–6061, doi:10.1016/j.atmosenv.2004.06.011, 2004.
Mann, G. W., Carslaw, K. S., Reddington, C. L., Pringle, K. J., Schulz, M., Asmi, A., Spracklen, D. V., Ridley, D. A., Woodhouse, M. T., Lee, L. A., Zhang, K., Ghan, S. J., Easter, R. C., Liu, X., Stier, P., Lee, Y. H., Adams, P. J., Tost, H., Lelieveld, J., Bauer, S. E., Tsigaridis, K., van Noije, T. P. C., Strunk, A., Vignati, E., Bellouin, N., Dalvi, M., Johnson, C. E., Bergman, T., Kokkola, H., von Salzen, K., Yu, F., Luo, G., Petzold, A., Heintzen-

ACPD
15, 26315–26355, 2015

berg, J., Clarke, A., Ogren, J. A., Gras, J., Baltensperger, U., Kaminski, U., Jennings, S. G., O'Dowd, C. D., Harrison, R. M., Beddows, D. C. S., Kulmala, M., Viisanen, Y., Ulevicius, V., Mihalopoulos, N., Zdimal, V., Fiebig, M., Hansson, H.-C., Swietlicki, E., and Henzing, J. S.: Intercomparison and evaluation of global aerosol microphysical properties among AeroCom models of a range of complexity, Atmos. Chem. Phys., 14, 4679–4713, doi:10.5194/acp-14-4679-2014, 2014.

Masalaite, A., Remeikis, V., Garbaras, A., Dudoitis, V., Ulevicius, V., and Ceburnis, D.: Elucidating carbonaceous aerosol sources by the stable carbon δ^{13}CTC ratio in size-segregated particles, Atmos. Res., 158–159, 1–12, doi:10.1016/j.atmosres.2015.01.014, 2015.

Matthew, B. M., Middlebrook, A. M., and Onasch, T. B.: Collection efficiencies in an aerodyne aerosol mass spectrometer as a function of particle phase for laboratory generated aerosols, Aerosol Sci. Tech., 42, 884–898, doi:10.1080/02786820802356797, 2008.

Middlebrook, A. M., Bahreini, R., Jimenez, J. L., and Canagaratna, M. R.: Evaluation of composition-dependent collection efficiencies for the Aerodyne aerosol mass spectrometer using field data, Aerosol Sci. Tech., 46, 258–271, doi:10.1080/02786826.2011.620041, 2012.

Mochida, M., Kawamura, K., Fu, P. Q., and Takemura, T.: Seasonal variation of levoglucosan in aerosols over the western North Pacific and its assessment as a biomass-burning tracer, Atmos. Environ., 44, 3511–3518, doi:10.1016/j.atmosenv.2010.06.017, 2010.

MODIS NASA LANCE – FIRMS: MODIS Active Fire Detections, Data set, available at: http://earthdata.nasa.gov/data/nrt-data/firms (last access: 6 June 2014), 2011.

Mohn, J., Szidat, S., Fellner, J., Rechberger, H., Quartier, R., Buchmann, B., and Emmenegger, L.: Determination of biogenic and fossil CO2 emitted by waste incineration based on $^{14}CO_2$ and mass balances, Bioresource Technol., 99, 6471–6479, doi:10.1016/j.biortech.2007.11.042, 2008.

Mohr, C., Huffman, J. A., Cubison, M. J., Aiken, A. C., Docherty, K. S., Kimmel, J. R., Ulbrich, I. M., Hannigan, M., and Jimenez, J. L.: Characterization of primary organic aerosol 25 emissions from meat cooking, trash burning, and motor vehicles with high-resolution aerosol mass spectrometry and comparison with ambient and chamber observations, Environ. Sci. Technol., 43, 2443–2449, doi:10.1021/es8011518, 2009.

Ng, N. L., Herndon, S. C., Trimborn, A., Canagaratna, M. R., Croteau, P. L., Onasch, T. B., Sueper, D., Worsnop, D. R., Zhang, Q., Sun, Y. L., and Jayne, J. T.: An Aerosol Chemical Speciation Monitor (ACSM) for routine monitoring of the composition and mass concentrations

ACPD
15, 26315–26355, 2015

of ambient aerosol, Aerosol Sci. Tech., 45, 770–784, doi:10.1080/02786826.2011.560211, 2011.
Oanh, N. T. K., Ly, B. T., Tipayarom, D., Manandhar, B. R., Prapat, P., Simpson, C. D., and Liu, L. J. S.: Characterization of particulate matter emission from open burning of rice straw, Atmos. Environ., 45, 493–502, doi:10.1016/j.atmosenv.2010.09.023, 2011.
Orasche, J., Schnelle-Kreis, J., Abbaszade, G., and Zimmermann, R.: Technical Note: In-situ derivatization thermal desorption GC-TOFMS for direct analysis of particle-bound non-polar and polar organic species, Atmos. Chem. Phys., 11, 8977–8993, doi:10.5194/acp-11-8977-2011, 2011.
Oros, D. R., Radzi bin Abas, M., Omar, N. Y. M. J., Rahman, N. A., and Simoneit, B. R. T.: Identification and emission factors of molecular tracers in organic aerosols from biomass burning: 3. Grasses, Appl. Geochem., 21, 919–940, doi:10.1016/j.apgeochem.2006.01.008, 2006.
Paatero, P.: Least squares formulation of robust non-negative factor analysis, Chemometr. Intell. Lab., 37, 23–35, doi:10.1016/S0169-7439(96)00044-5, 1997.
Paatero, P. and Tapper, U.: Positive matrix factorization – a nonnegative factor model with optimal utilization of error-estimates of data values, Environmetrics, 5, 111–126, doi:10.1002/env.3170050203, 1994.
Paatero, P., Eberly, S., Brown, S. G., and Norris, G. A.: Methods for estimating uncertainty in factor analytic solutions, Atmos. Meas. Tech., 7, 781–797, doi:10.5194/amt-7-781-2014, 2014.
Popovicheva, O., Kistler, M., Kireeva, E., Persiantseva, N., Timofeev, M., Kopeikin, V, and Kasper-Giebl, A.: Physicochemical characterization of smoke aerosol during large-scale wildfires: extreme event of August 2010 in Moscow, Atmos. Environ., 96, 405–414, doi:10.1016/j.atmosenv.2014.03.026, 2014.
Puxbaum, H., Caseiro, A., Sánchez-Ochoa, A., Kasper-Giebl, A., Claeys, M., Gelencsér, A., Legrand, M., Preunkert, S., and Pio, C.: Levoglucosan levels at background sites in Europe for assessing the impact of biomass combustion on the European aerosol background, J. Geophys. Res., 112, D23S05, doi:10.1029/2006JD008114, 2007.
Reid, J. S., Prins, E. M., Westphal, D. L., Schmidt, C. C., Richardson, K. A., Christopher, S. A., Eck, T. F., Reid, E. A., Curtis, C. A., and Hoffman, J. P.: Real-time monitoring of South American smoke particle emissions and transport using a coupled remote sensing/box-model approach, Geophys. Res. Lett., 31, L06107, doi:10.1029/2003GL018845, 2004.

ACPD
15, 26315–26355, 2015

Saarikoski, S., Sillanpaa, M., Sofiev, M., Timonen, H., Saarnio, K., Teinela, K., Karppinen, A., Kukkonen, J., and Hillamo, R.: Chemical composition of aerosols during a major biomass burning episode over northern Europe in spring 2006: experimental and modelling assessments, Atmos. Environ., 41, 3577–3589, doi:10.1016/j.atmosenv.2006.12.053, 2007.

Salazar, G., Zhang, Y. L., Agrios, K., and Szidat, S.: Development of a method for fast and automatic radiocarbon measurement of aerosol samples by online coupling of an elemental analyzer with a MICADAS AMS, Nucl. Instrum. Meth. B., in press, doi:10.1016/j.nimb.2015.03.051, 2015.

Schmidl, C., Marr, I. L., Caseiro, A., Kotianová, P., Berner, A., Bauer, H., Kasper-Giebl, A., and Puxbaum, H.: Chemical characterisation of fine particle emissions from wood stove combustion of common woods growing in mid-European Alpine regions, Atmos. Environ., 42, 126–141, doi:10.1016/j.atmosenv.2007.09.028, 2008.

Sullivan, A. P., Holden, A. S., Patterson, L. A., McMeeking, G. R., Kreidenweis, S. M., Malm, W. C., Hao, W. M., Wold, C. E., and Collett Jr., J. L.: A method for smoke marker measurements and its potential application for determining the contribution of biomass burning from wildfires and prescribed fires to ambient $PM_{2.5}$ organic carbon, J. Geophys. Res., 113, D22302, doi:10.1029/2008JD010216, 2008.

Sun, Y. L., Wang, Z. F., Dong, H. B., Yang, T., Li, J., Pan, X. L., Chen, P., and Jayne, J. T.: Characterization of summer organic and inorganic aerosols in Beijing, China with an Aerosol Chemical Speciation Monitor, Atmos. Environ., 51, 250–259, doi:10.1016/j.atmosenv.2012.01.013, 2012.

Szidat, S., Jenk, T. M., Gäggeler, H. W., Synal, H.-A., Fisseha, R., Baltensperger, U., Kalberer, M., Samburova, V., Reimann, S., Kasper-Giebl, A., and Hajdas, I.: Radiocarbon (^{14}C)-deduced biogenic and anthropogenic contributions to organic carbon (OC) of urban aerosols from Zurich, Switzerland, Atmos. Environ., 38, 4035–4044, doi:10.1016/j.atmosenv.2004.03.066, 2004.

Szidat, S., Salazar, G. A., Vogel, E., Battaglia, M., Wacker, L., Synal, H.-A., and Türler, A.: ^{14}C analysis and sample preparation at the new Bern Laboratory for the Analysis of Radiocarbon with AMS (LARA), Radiocarbon, 56, 561–566, doi:10.2458/56.17457, 2014.

Timonen, H., Aurela, M., Carbone, S., Saarnio, K., Saarikoski, S., Mäkelä, T., Kulmala, M., Kerminen, V.-M., Worsnop, D. R., and Hillamo, R.: High time-resolution chemical characterization of the water-soluble fraction of ambient aerosols with PILS-TOC-IC and AMS, Atmos. Meas. Tech., 3, 1063–1074, doi:10.5194/amt-3-1063-2010, 2010.

ACPD
15, 26315–26355, 2015

Turekian, V. C., Macko, S., Ballentine, D., Swap, R. J., and Garstang, M.: Causes of bulk carbon and nitrogen isotopic fractionations in the products of vegetation burns: laboratory studies, Chem. Geol., 152, 181–192, doi:10.1016/S0009-2541(98)00105-3, 1998.

Ulbrich, I. M., Canagaratna, M. R., Zhang, Q., Worsnop, D. R., and Jimenez, J. L.: Interpretation of organic components from Positive Matrix Factorization of aerosol mass spectrometric data, Atmos. Chem. Phys., 9, 2891–2918, doi:10.5194/acp-9-2891-2009, 2009.

Ulevicius, V., Mordas, G., and Plauskaite, K.: Evolution of aerosol particle size distribution in the coastal environment: Effect of relative humidity, SO_2 and NO_2, Environ. Chem. Phys., 24, 13–17, 2002.

Ulevicius, V., Byčenkienė, S., Remeikis, V., Garbaras, A., Kecorius, S., Andriejauskienė, J., Jasinevičienė, D., and Močnik, G.: Characterization of aerosol particle episodes in Lithuania caused by long-range and regional transport, Atmos. Res., 98, 190–200, doi:10.1016/j.atmosres.2010.03.021, 2010a.

Ulevicius, V., Byčenkienė, S., Špirkauskaitė, N., and Kecorius, S.: Biomass burning impact on black carbon aerosol mass concentration at a coastal site: case studies, Lith. J. Phys., 50, 335–344, doi:10.3952/lithjphys.50304, 2010b.

Weimer, S., Alfarra, M. R., Schreiber, D., Mohr, M., Prevot, A. S. H., and Baltensperger, U.: Organic aerosol mass spectral signatures from wood burning emissions: influence of burning conditions and wood type, J. Geophys. Res., 113, D10304, doi:10.1029/2007JD009309, 2008.

Widory, D.: Nitrogen isotopes: Tracers of origin and processes affecting PM_{10} in the atmosphere of Paris, Atmos. Environ., 41, 2382–2390, doi:10.1016/j.atmosenv.2006.11.009, 2007.

Yttri, K. E., Simpson, D., Nøjgaard, J. K., Kristensen, K., Genberg, J., Stenström, K., Swietlicki, E., Hillamo, R., Aurela, M., Bauer, H., Offenberg, J. H., Jaoui, M., Dye, C., Eckhardt, S., Burkhart, J. F., Stohl, A., and Glasius, M.: Source apportionment of the summer time carbonaceous aerosol at Nordic rural background sites, Atmos. Chem. Phys., 11, 13339–13357, doi:10.5194/acp-11-13339-2011, 2011.

Zawadzka, O., Makuch, P., Krzysztof, M, Markowicz., Zieliński, T., Petelski, T., Ulevicius, V., Strzałkowska, A., Rozwadowska, A., and Gutowska, D.: Studies of aerosol optical depth with the use of microtops II sun photometers and MODIS detectors in coastal areas of the Baltic Sea, Acta Geophys., 62, 400–422, doi:10.2478/s11600-013-0182-5, 2013.

Zhang, Y. L., Perron, N., Ciobanu, V. G., Zotter, P., Minguillón, M. C., Wacker, L., Prévôt, A. S. H., Baltensperger, U., and Szidat, S.: On the isolation of OC and EC and the optimal strategy of

ACPD
15, 26315–26355, 2015

radiocarbon-based source apportionment of carbonaceous aerosols, Atmos. Chem. Phys., 12, 10841–10856, doi:10.5194/acp-12-10841-2012, 2012.

Zhang, Y.-L., Huang, R.-J., El Haddad, I., Ho, K.-F., Cao, J.-J., Han, Y., Zotter, P., Bozzetti, C., Daellenbach, K. R., Canonaco, F., Slowik, J. G., Salazar, G., Schwikowski, M., Schnelle-Kreis, J., Abbaszade, G., Zimmermann, R., Baltensperger, U., Prévôt, A. S. H., and Szidat, S.: Fossil vs. non-fossil sources of fine carbonaceous aerosols in four Chinese cities during the extreme winter haze episode of 2013, Atmos. Chem. Phys., 15, 1299–1312, doi:10.5194/acp-15-1299-2015, 2015.

Zotter, P., Ciobanu, V. G., Zhang, Y. L., El-Haddad, I., Macchia, M., Daellenbach, K. R., Salazar, G. A., Huang, R.-J., Wacker, L., Hueglin, C., Piazzalunga, A., Fermo, P., Schwikowski, M., Baltensperger, U., Szidat, S., and Prévôt, A. S. H.: Radiocarbon analysis of elemental and organic carbon in Switzerland during winter-smog episodes from 2008 to 2012 – Part 1: Source apportionment and spatial variability, Atmos. Chem. Phys., 14, 13551–13570, doi:10.5194/acp-14-13551-2014, 2014.

ACPD
15, 26315–26355, 2015

Table 1. Preila site surroundings 10 km.

Site altitude	5 (m) a.s.l.	Terrain below site	50.0 (%)
Median altitude	0 (m) a.s.l.	Standard deviation of altitude	7 (m)
Total population	6831	Standard deviation of population	159
Mean population density	20 (km^{-2})	Standard deviation of population	13 (km^{-2})
Local population density	29.5 (km^{-2})	density	
Dominating land cover types (based on GLC2000)			
Water bodies (natural and artificial) (20)			84.9 (%)
Tree cover, needle-leaved, evergreen (4)			13.2 (%)
Tree cover, mixed leaf type (6)			1.1 (%)
Herbaceous cover, closed-open (13)			0.4 (%)

ACPD
15, 26315–26355, 2015

Table 2. Variation of the fractions of EC_f, EC_{nf}, OC_f, OC_{nf} and TC, EC and OC values during the study periods.

$\mu g\,m^{-3}$/date of collection	EC_f	EC_{nf}	OC_f	OC_{nf}	TC	EC	OC
5 Mar 2014	0.25 ± 0.04	0.33	0.47 ± 0.10	2.34 ± 0.18	3.39 ± 0.18	0.59 ± 0.17	2.80 ± 0.18
7 Mar 2014	0.21 ± 0.04	0.61	0.39 ± 0.12	2.80 ± 0.20	4.01 ± 0.23	0.81 ± 0.24	3.31 ± 0.20
8 Mar 2014	0.15 ± 0.05	0.26	0.56 ± 0.07	1.46 ± 0.12	2.43 ± 0.13	0.41 ± 0.18	2.24 ± 0.15
9 Mar 2014	0.46 ± 0.16	0.95	0.95 ± 0.18	4.98 ± 0.36	7.28 ± 0.43	1.36 ± 0.63	6.32 ± 0.35
10 Mar 2014	0.56 ± 0.18	1.64	1.64 ± 0.28	7.77 ± 0.50	11.72 ± 0.64	2.31 ± 0.75	9.47 ± 0.51

ACPD
15, 26315–26355, 2015

Table 3. Average percentage contributions of different sources.

Relative contributions [%] to TC	POC_f	POC_{nf}	SOC_f	SOC_{nf}	EC_f	EC_{nf}	TC to PM_1
5 Mar 2014	5.07	43.23	6.69	22.51	9.66	12.83	28.44
7 Mar 2014	6.26	43.58	5.66	19.14	6.58	18.79	37.62
8 Mar 2014	7.73	26.28	13.36	18.65	12.60	21.38	24.80
9 Mar 2014	4.55	41.30	4.38	13.12	12.48	24.17	51.27
10 Mar 2014	6.82	43.02	5.9	14.83	7.18	22.26	43.91
Relative contributions [%] to OC	POC_f	POC_{nf}	SOC_f	SOC_{nf}			
5 Mar 2014	6.55	55.78	8.63	29.04			
7 Mar 2014	8.39	58.38	7.59	25.64			
8 Mar 2014	11.70	39.80	20.24	28.25			
9 Mar 2014	7.18	65.20	6.91	20.71			
10 Mar 2014	9.66	60.96	8.36	21.02			

ACPD
15, 26315–26355, 2015

Figure 1. (a) Map of the observation site, Preila (indicated by the red marker). Nearest major cities are Klaipeda (40 km north) and Kaliningrad (90 km south), **(b)** Environmental pollution research station Preila and site surroundings **(c)**.

ACPD
15, 26315–26355, 2015

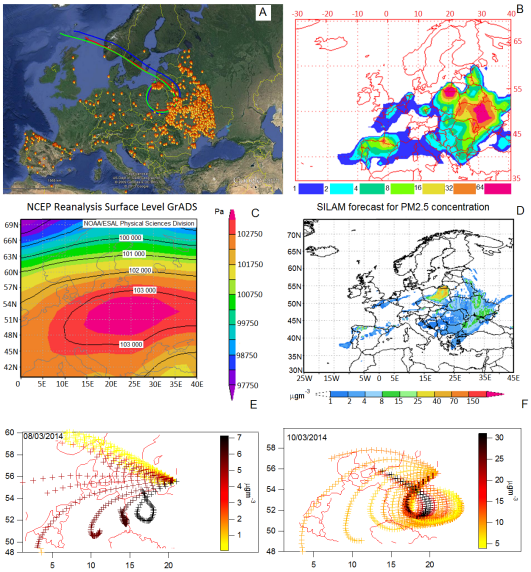

Figure 2. (a) Combined MODIS images observed from the Aqua satellite on 10 March 2014, showing numerous fires due to seasonal grass burning and 72 h air mass backward trajectories from the fire regions arriving at Preila at 100 (red), 200 (blue) and 500 (green) m a.g.l. (AGL). **(b)** NAAPS model results showing surface smoke concentrations for the strongest stage (10 March 2014) (the color scale (from blue to purple) corresponds to the 7 levels of the contours that indicate the smoke mass mixing ratio ($\mu g\,m^{-3}$) at the surface). Smoke optical depth at a wavelength of 0.55 microns. The contouring begins at 1 $\mu g\,m^{-3}$ and doubles in magnitude for each successive contour. **(c)** Pressure level at surface at 2.5° latitude × 2.5° longitude global grids in Pa (NCEP/NCAR Reanalysis 1, 10 March 2014). **(d)** $PM_{2.5}$ concentration ($\mu g\,m^{-3}$) forecast utilized by the SILAM chemical transport model during the event of grass fires, (**e** and **f**) ACSM organic concentration ACSM organics concentration ($\mu g\,m^{-3}$) (measured in Preila) weighted air mass back trajectories of 48 h (an arrival on 8 (left) and 10 (right) March 2014) with an altitude endpoint of 500 m a.g.l.

ACPD
15, 26315–26355, 2015

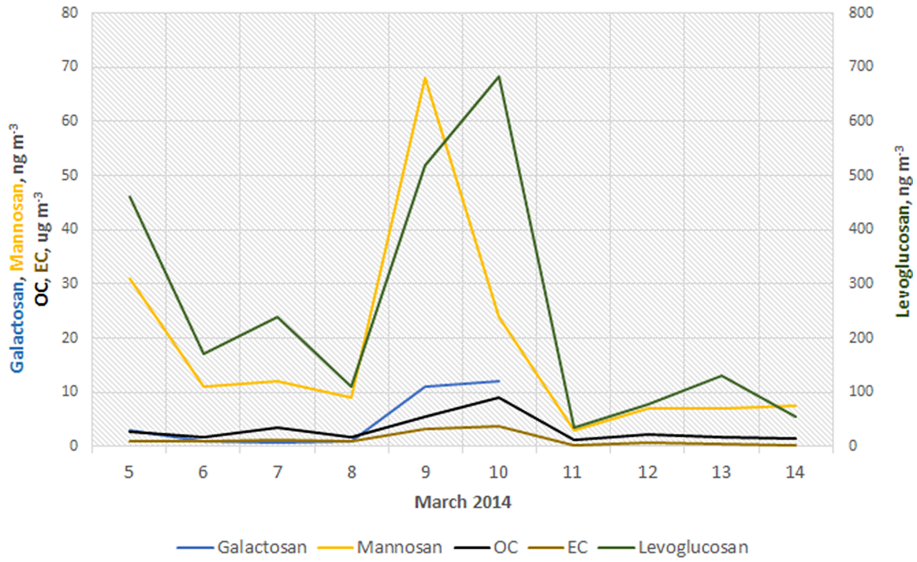

Figure 3. Averaged concentrations between daily values from 5 to 14 March 2014 for levoglucosan, galactosan, mannosan (in ng m^{-3}) and for elemental carbon (EC) and organic carbon (OC) in µg m^{-3}.

ACPD
15, 26315–26355, 2015



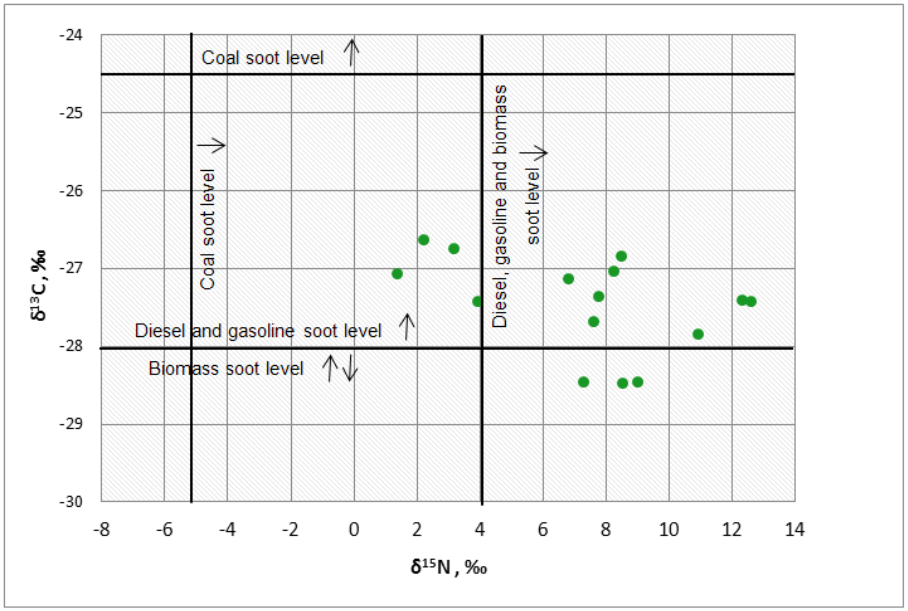

Figure 4. Stable carbon and nitrogen isotope ratio values of PM_1 in Preila station. Vertical and horizontal lines represent carbon and nitrogen, respectively, isotope ratio characteristic values for the sources of aerosol particles (Garbaras et al., 2008, 2015; Ulevicius et al., 2010a; Widory, 2007).

ACPD
15, 26315–26355, 2015

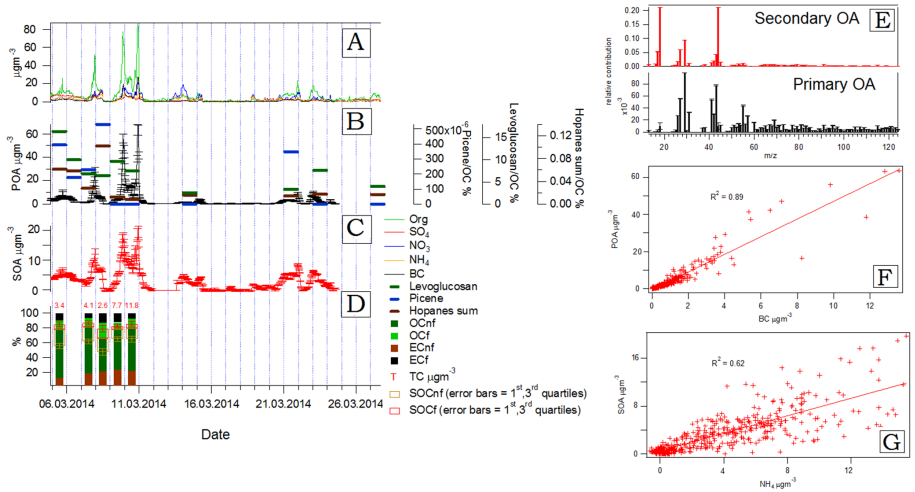

Figure 5. Average chemical composition and time series of NR-PM_1 OA for the entire study **(a)**, **(b)** Time series of the POA factor and percent contribution of the corresponding tracer species (levoglucosan, picene and hopanes) to total OA, **(c)** Time series of the SOA factor, **(d)** Relative source apportionment of TC during BB event. Numbers indicate the total carbon absolute concentrations in $\mu g\,m^{-3}$, variations of the mass concentrations of the SOC_f and SOC_{nf} (the whiskers above and below the boxes indicate the 1st and 3rd quartiles, **e**) Mass spectra of SOA and POA, error bars represent the standard deviation of 20 PMF runs, **(f–g)** The scatter plots illustrate the relationship between SOA and NH_4^+ **(f)** and sum of SO_4^{2-} and NO_3^- with NH_4^+ **(g)**.

ACPD
15, 26315–26355, 2015

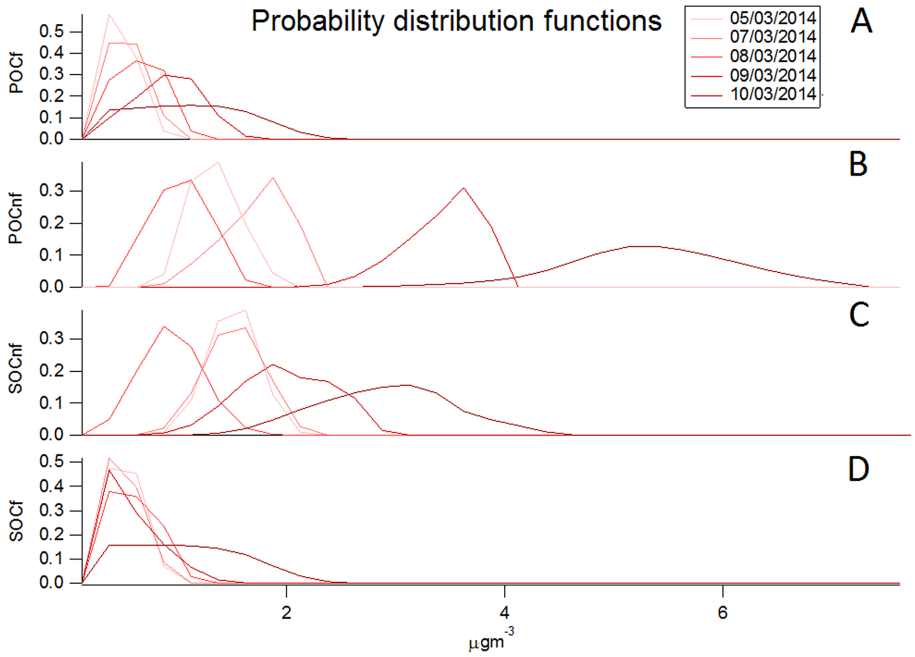

Figure 6. Probability distribution functions of the absolute daily contribution of POC_f **(a)**, POC_{nf} **(b)**, SOC_{nf} **(c)**, SOC_f **(d)**.

ACPD
15, 26315–26355, 2015

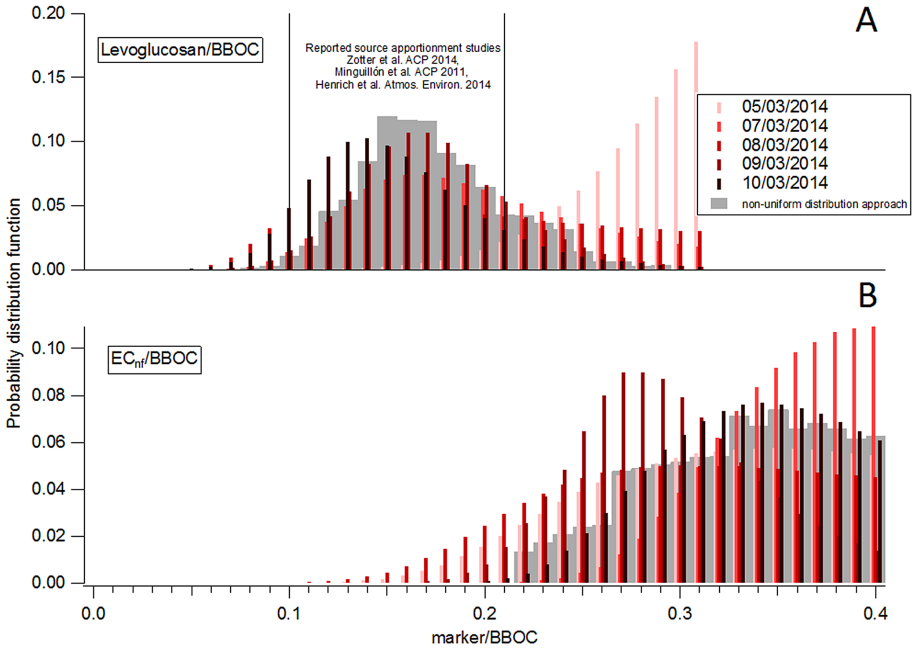

Figure 7. Probability distribution functions of Levoglucosan/BBOC **(a)** and EC_{nf}/BBOC **(b)**.

ACPD
15, 26315–26355, 2015